

Solvothermal synthesis and characterization of a new 3D potassium Metal-Organic Framework (MOF) structure.

O. S. Bull*

Department of Chemistry, Rivers state University of Science and Technology, Nkpolu-Oroworukwo, Port Harcourt.

*corresponding author: bull.okpara@ust.edu.ng

Received 25 November 2019; accepted 02 January 2020, published online 07 February 2020

Abstract:

Novel 3-D potassium- containing material $[K(dhbdca)_{0.5}]$, named RSUST-1 was synthesised solvothermally using 2,5-dihydroxy-benzene-1,4-dicarboxylic acid (dhbdca) as ligand in a 1:1 H_2O/DMA solvent mixture. The new material synthesised has been structurally characterised by means of single crystal X-ray diffraction, powder X-ray diffraction, infra-red spectroscopy, elemental analysis and thermogravimetric analysis (TGA). The single crystal X-ray diffraction studies show that $[K(dhbdca)_{0.5}]$ crystallize in the monoclinic $P2(1)/n$, space groups. The thermogravimetric analysis shows that the compound is thermally stable over a wide range of temperatures.

Keywords: solvothermal Synthesis, Metal- Organic Framework structures, 3D metal structures.

Introduction.

Over the past few years, many Metal- Organic Frameworks (MOFs) have been prepared in order to study their micro-porous frameworks, thermal stability and potential application in gas storage, catalytic heterogeneous reactions, non-linear optics, electronics and separation techniques such as ion exchange [1-7]. A successful approach to obtaining a MOF depends on the choice of the building units which have significant influence on the topological structure and functionality of MOFs. Bridging ligands are important building units in the construction of MOFs. Hence, to control the structure of a MOF material, the selection of rigid, organic linkers is one of the most crucial decisions. For this reason, most of the organic linkers used in the construction of MOFs are usually molecules containing aromatic groups that give rigidity to the MOF network. The functional groups in the aromatic organic ligand could be carboxylic acid, [8-14] heterocyclic aromatic rings containing N atoms (pyridine) [15–19] or other coordinating functional groups such as phosphonates^{18–22} and sulfonate [23,24]. In theory the structure as well as the properties of a MOF can be pre-designed and systematically tuned using a suitable selection of the building blocks. Apart from predesigned synthesis of MOFs, post-design synthesis of MOFs has

also been successfully used in modifying or tuning the pore properties of MOFs [25,26]. Unlike other well-known porous materials such as zeolite and activated carbons, the facile tune-ability of MOFs can in some cases make it easy for the optimization of their structure, surface functionalization as well as other prerequisite properties for specific application as porous material [27].

Rigid MOFs are characterized by the fact that they possess a comparatively stable and robust porous framework with permanent porosity comparable to that of zeolite, whereas flexible MOFs have frameworks that respond to factors such as temperature and pressure as well as guest molecules. The special sensitivity of MOFs to temperature or pressure makes them outstanding for temperature/pressure molecular sieving which other traditional adsorbents like zeolites and activated carbons lack. Thus the intense current research efforts towards the industrial application of MOFs in gas separation and storage as well as in catalysis is attributed to their robustness, unique structural properties such as high thermal and chemical stability, unprecedented internal surface areas of up to 5000 m²/g, high void volumes of 55-90% as well as low density from 0.21-1.00 g/cm³, which can be sustained upon the removal of guest molecules such as H₂O from the pores.¹ The rapid number of related research publications in

recent years is indicative of the importance of MOFs as CO₂ adsorbent [28,29]. However, most MOFs are constructed with transition metals or rare earth metals that are relatively toxic, expensive and heavy weight when compared to alkali metals or alkaline-earth metals. There is a dearth of literature of s-block element MOFs, of which their light, less toxic and less expensive nature have priority in constructing frameworks materials with light volumetric and novel topology for a myriad of applications.

Experimental Section

All solvents and reagents in this work were used as received without further purification. Infra-red spectroscopic studies were recorded on a Perkin Elmer Spectrum 100 FT-IR Spectrometer. Single crystal X-ray diffraction was carried out on an Oxford Diffraction Xcalibur PX Ultra diffractometer. Powder X-ray diffraction was carried out on a Phillips PW1700 series automated powder X-ray diffractometer. TGA was carried out on a Perkin Pyris 1 machine which was under a constant nitrogen gas flow rate of 20.0 ml/min and temperature range of 25-700 °C and heating rate of 10.00 °C/min. Elemental analysis was also done. The oven used was a Memmert thermostat universal oven UNE 200-800, UFE 400-800.

RSUST-1 was synthesised using a mixture of dimethylacetamide (DMA) and water (1:1) with 2.5 mmol (0.4953 g) of 2,5-dihydroxybenzene-1,4-dicarboxylic acid (dhbdca) and KNO₃ 5.0 mmol (0.505 g) was put in a clean beaker and stirred for 10 minutes using a magnetic stirrer at 120 °C. The resulting pale brown solution was transferred into a Teflon

lined autoclave and firmly sealed. The firmly closed autoclave was put in to an oven and heated at 120 °C for 24 h and allowed to cool slowly for 6 h to obtain colourless block crystalline material at the bottom of the autoclave. The solvent in the autoclave was decanted and the crystalline material was dried in the fume cupboard under ambient conditions. The percentage yield based on the metal salt was 82%.

Results and discussion

RSUST-1 crystallizes in the monoclinic crystal system and space group of P2(1)/n with a molecular formula of C₄H₂KO₃. The crystals are pale yellow plates in nature. There are seven linkages to the metal centre K1 and the coordination pattern to the metal centre is the same as mode A- Fig1 [30]. The only difference is that in addition to the COOH groups, the OH groups of the alcoholic functional groups in the ligand (dhbdca) were also involved in the bonding that resulted into the formation of RSUST-1. Five of these bonds are from the carboxylate functional group of the ligand (dhbdca) and the other two are from the alcoholic functional group of the ligand (dhbdca). These linkages are properly shown in Figure 2 as well as how the linkages led to the formation of a 3-D framework with lots of open channels in Figure 3. Thus, two K metals centres are bridged in a syn-syn mode which could be described as $\eta^1:\eta^2:\mu_2$ thereby forming the dinuclear unit. The bond length of the K-O from the carboxylate functional group ranges from 2.6773(14)-2.9485(14) whereas those from the OH of the alcoholic group ranges from 2.7473(14)-2.8017(15). Few selected data of the Single crystal X-ray diffraction are displayed (Table 1).

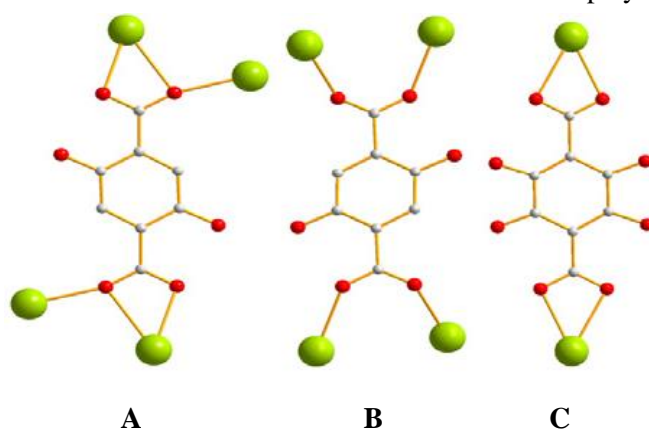


Fig. 1: Three coordination mode of dhbdca linker.¹³

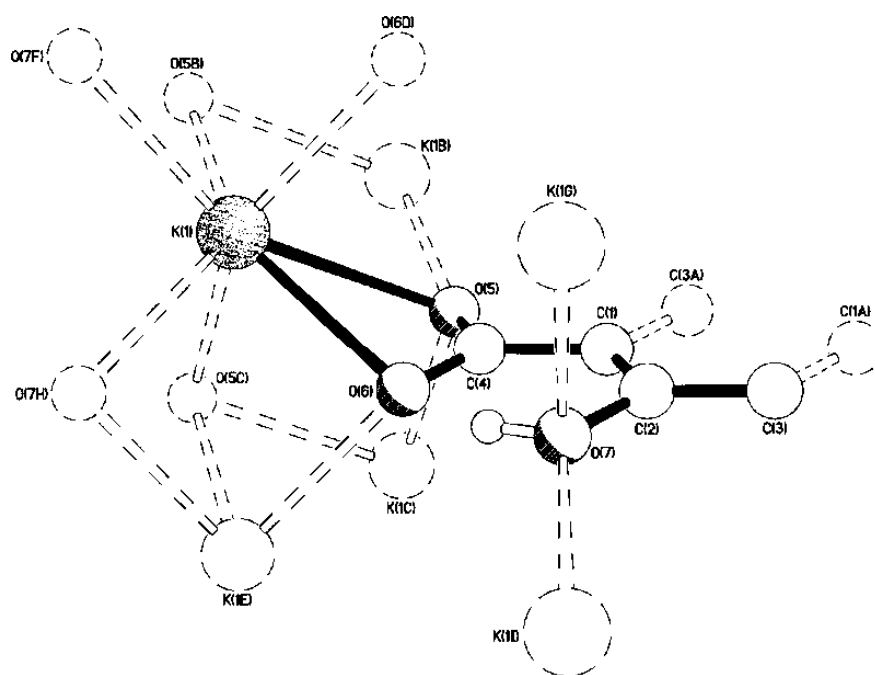


Fig. 2: Projection of the single crystal X-ray diffraction of RSU-1 $\{K(dhbdca)_{0.5}\}$ with atoms labelled showing the coordination environment of the K metal centre.

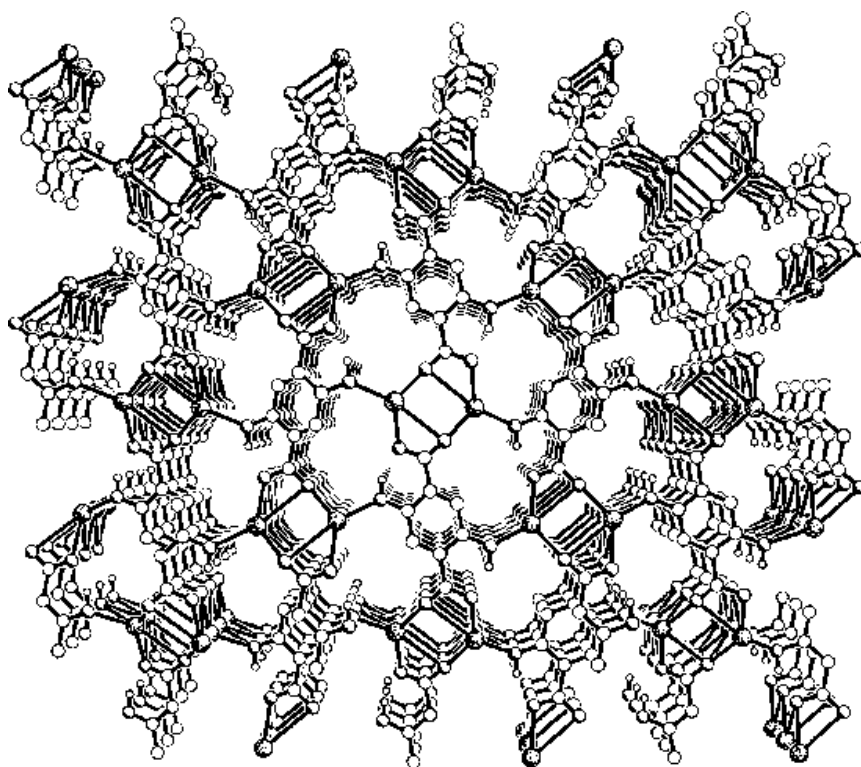


Fig. 3: Linkages of dhbdca with the metal centre (K) to form RSUST-1 with a 3-D framework and porosity.

Table 1. Crystal data and structure refinement for RSUST-1.

Identification code	RSUST-1
Formula	C ₄ H ₂ K O ₃
Formula weight	137.16
Temperature	173 K
Diffractometer, wavelength	OD Xcalibur 3, 0.71073 Å
Crystal system, space group	Monoclinic, P2(1)/n
Unit cell dimensions	a = 3.70752(19) Å α = 90° b = 10.4459(5) Å β = 95.346(5)° c = 12.2328(6) Å γ = 90°
Volume, Z	471.70(4) Å ³ , 4
Density (calculated)	1.931 Mg/m ³
Absorption coefficient	1.013 mm ⁻¹
F(000)	276
Crystal colour / morphology	Pale yellow plates
Crystal size	0.47 x 0.32 x 0.03 mm ³
□ range for data collection	3.35 to 32.60°
Index ranges	-5<=h<=3, -15<=k<=15, -18<=l<=18
Reflns collected / unique	2375 / 2375 [R(int) = 0.0000]
Reflns observed [F>4σ(F)]	2088
Absorption correction	Analytical
Max. and min. transmission	0.973 and 0.702
Refinement method	Full-matrix least-squares on F ²
Data / restraints / parameters	2375 / 1 / 78
Goodness-of-fit on F ²	1.050
Final R indices [F>4σ(F)]	R1 = 0.0398, wR2 = 0.1243
R indices (all data)	R1 = 0.0473, wR2 = 0.1280
Largest diff. peak, hole	0.542, -0.753 eÅ ⁻³
Mean and maximum shift/error	0.000 and 0.000

Table 2. Bond lengths [Å] and angles [°] for PDL1211.

K(1)-O(5)#1	2.6773(14)
K(1)-O(7)#2	2.7473(14)
K(1)-O(6)	2.7697(14)
K(1)-O(5)#3	2.7803(15)
K(1)-O(7)#4	2.8017(15)
K(1)-O(6)#5	2.8026(14)
K(1)-O(5)	2.9485(14)
O(5)-K(1)#1	2.6773(14)
O(5)-K(1)#3	2.7803(15)
O(6)-K(1)#7	2.8026(14)
O(7)-K(1)#8	2.7473(14)
O(7)-K(1)#9	2.8017(15)

Symmetry transformations used to generate equivalent atoms:

- #1 -x,-y,-z #2 -x+3/2,y-1/2,-z+1/2 #3 -x+1,-y,-z
 #4 -x+1/2,y-1/2,-z+1/2 #5 x-1,y,z #6 -x+1,-y+1,-z
 #7 x+1,y,z #8 -x+3/2,y+1/2,-z+1/2 #9 -x+1/2,y+1/2,-z+1/2

Powder X-ray Diffraction of RSUST-1.

Other than single crystal X-ray diffraction studies of RSUST-1, Powder X-ray

diffraction was also carried out on RSUST-1 as shown in Figure 4.

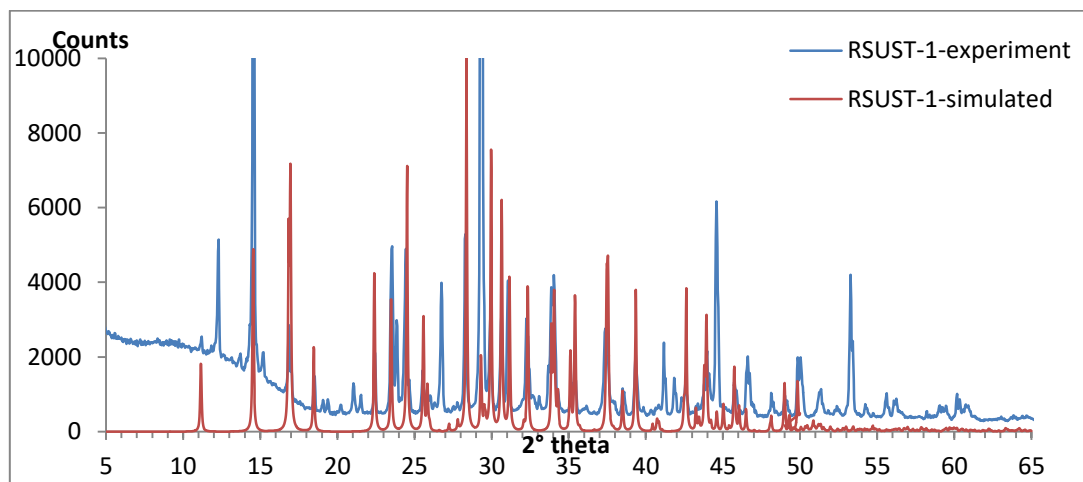


Fig. 4: Powder X-ray pattern of RSUST-1 compound showing the stacking of experimental and simulated patterns.

The experimental X-ray diffraction is stacked into the simulated X-ray diffraction from single crystal X-ray diffraction. As can be seen from Figure 3 above the fitting is not good. Some peaks appear in both patterns others do not. This could be a result of uneven grinding of the sample into powder or indicative of the presence of impurity, or maybe lack of quality crystals. The elemental analysis for RSUST-1 gives more detailed information about its purity as shown on **Table 2**.

Table 2: Elemental analysis of RSUST-1 plus H₂O.

Compound	%C		%H	
	Expected	Found	Expected	Found
RSUST-1	30.93	30.44	2.60	2.76

Thermogravimetric Analysis of RSUST-1

The thermal behaviour of RSUST-1 was also investigated. From the single crystal X-ray diffraction structures displayed in Fig 2, it is expected that RSUST-1 will be stable to a high degree then lose the organic moiety to form a stable metal carbonate (K₂CO₃) or the metal oxide (K₂O). However, as indicated in Table 2, if the sample contained some water as a result of uneven drying then there will be a slow drop in step-**Fig. 5**.

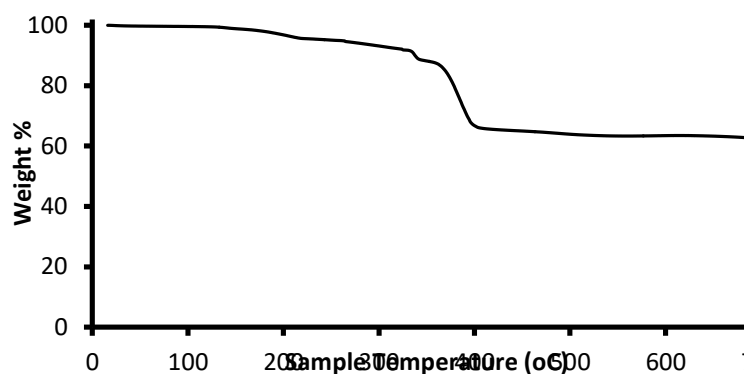


Fig. 5: Thermogravimetric Analysis of RSUST-1.

From the TGA plot, the thermal behaviour of RSUST-1 shows a slow drop in weight to about 88.41% and 346°C on the weight and temperature axis respectively. This loss is attributed to the water molecule added because the sample was not evenly dried thus resulting into an 11.59% weight loss which agrees with expected calculated value of 11.61%. Thereafter the compound begins to lose its organic moiety to form the metal oxide (K_2O) at about 68.51% and 394°C on the weight and temperature axis respectively. This results into a weight loss of 31.49% based on X-ray + H_2O which is

in harmony with calculated weight loss of the organic moiety of 31.32%.

Infra-red spectroscopic studies on RSUST-1

The IR of RSUST-1 (Fig 6b) shows an OH stretch at 3128 cm^{-1} , a CO asymmetric stretch at 1631 cm^{-1} , CO symmetric stretch at 1511 cm^{-1} and aromatic C=C peak at 1458 cm^{-1} . A comparison of the spectra of the dhdca (Fig 6a) and the RSUST-1 confirmed the presence of the ligand in RSUST-1 implying the incorporation of the ligand in the MOF.

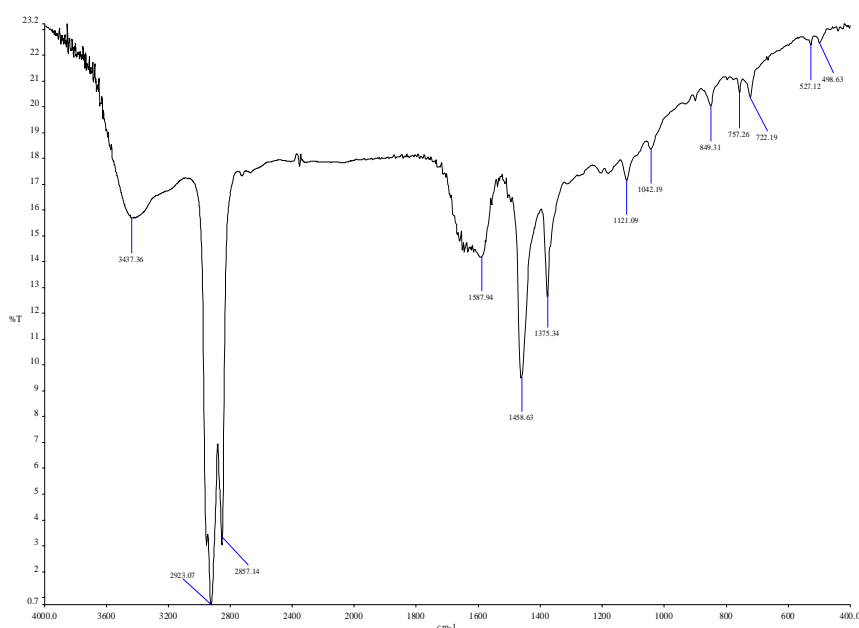


Fig. 6a: IR Spectrum of 2,5-dihydroxy-benzene-1,4-dicarboxylic acid (dhdca)

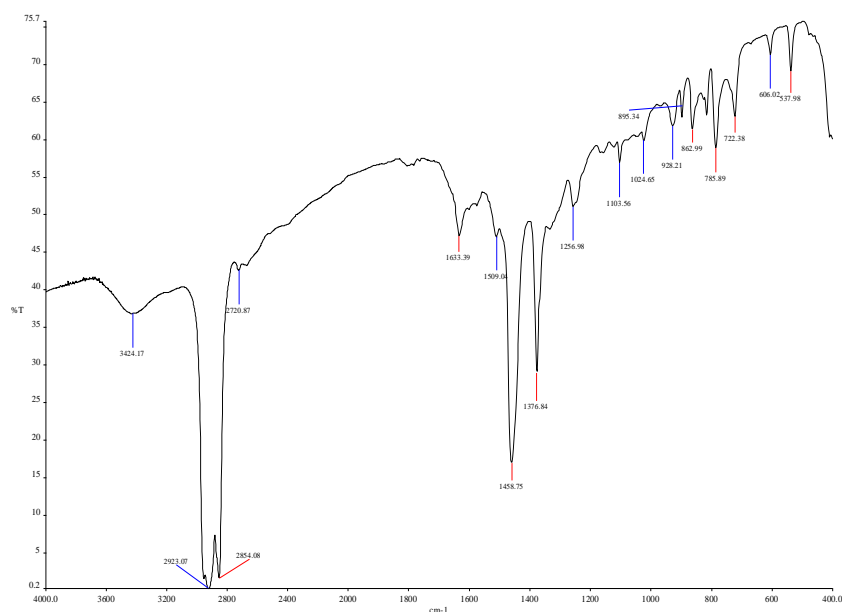


Fig. 6b: IR Spectrum of RSUST-1

Conclusion

The novel 3-D framework material, RSUST-1, has been synthesised solvothermally using 2,5-dihydroxy benzene 2,4-dicarboxylic acid (dhbdca) as ligand in a water/DMA solvent mixture. The characterization of this novel 3-D framework material by means of single crystal X-ray diffraction, powder X-ray diffraction, elemental analysis, TGA and IR has led to the determination of the coordination environment

around the metal centres, the purity of the framework material as well as other physicochemical properties. The elemental analysis of RSUST-1 shows that the framework material is free of impurities.

References.

- [1] M. Eddaoudi, J. Kim, N. Rosi, D. Vodak, J. Wachter, M. O'Keeffe and O. M. Yaghi (2002), Systematic design of pore size and functionality of isorecticular MOFs and their application in methane storage, *Science*, **295**, 469-472.
- [2] H.K. Chae, D.Y. Siberio-Perez, J. Kim, Y. Go, M. Eddaoudi, A.J. Matzger, M. O'Keeffe, O.M. Yaghi (2004), A route to high surface area, porosity and inclusion of large molecules in crystals, *Nature*, **427**, 523-527.
- [3] X.Q. Lu, J.J. Jiang, C. H. Chen, B.S. Kang, C.Y. Su (2005), 3D coordination polymers with nitrilotriacetic and 4,4'-bipyridyl mixed ligands: structural variation based on dinuclear or tetranuclear subunits assisted by Na-O and /or O... *Inorganic Chemistry*, **44**, 4515-4521.
- [4] G. Ferey, C. Mellot-Draznieks, C. Serre, F. Millange, J. Dutour, S. Surble, I. Margiolaki (2005), A chromium terephthalate-based solid with unusually

- large pore volumes and surface area, *Science*, **309**, 2040-2054.
- [5] D.N. Dybtsev, H. Chun, S.H. Yoon, D. Kim, K. Kim (2004), Microporous manganese formate: a simple metal-organic porous material with high framework stability and highly selective gas sorption properties, *Journal of the American Chemical Society*, **126**, 32-33.
- [6] H. Li, M. Eddaoudi, D.A. Richardson, O.M. Yaghi (1998), Porous Germanates: Synthesis, structure, and inclusion properties of $\text{Ge}_7\text{O}_{14.5}\text{F}_2[(\text{CH}_3)_2\text{NH}_2]_3(\text{H}_2\text{O})_{0.86}$ *Journal of the American Chemical Society*, **120**, 8567-8568.
- [7] D. Maspoch, D. Ruiz-Molina, K. Wurst, N. Domingo, M. Cavallini, F. Biscarini, J. Tejada, C. Rovira, J. Veciana (2003), A nanoporous molecular and magnet with reversible solvent-induced and mechanical and magnetic properties. *Nature Materials*, **2**, 190-195.
- [8] H. Li, M. Eddaoudi, M. O'Keeffe and O. M. Yaghi (1999), Design and synthesis of an exceptionally stable and highly porous metal-organic framework, *Nature*, **402**, 276-279.
- [9] C.Y. Liu, Y.Q. Ma, H.R. Tian, C.Y. Gao, Y.H. Li and Z.M. Sun (2017), A novel Cd(II)-MOF constructed from an organosilicon tetracarboxylic acid ligand Chinese Journal of Structural Chemistry. **36**, 654-660.
- [10] A. Vlad, M.-F. Zaltariov, S. Shova, G. Novitchi, C. Train and M. Cazacu (2016), Metal-organic frameworks based on tri- and penta-nuclear manganese (II) secondary building units self-assembled by a V-shaped silicon-containing dicarboxylate RSC Advances., **6**, 37412-37423.
- [11] R. P. Davies, R. J. Less, P. D. Lickiss and A. J. P. White (2007), Framework materials assembled from magnesium carboxylate building units, *Dalton Transactions*, **3**, 2528-2535.
- [12] R. P. Davies, R. Less, P. D. Lickiss, K. Robertson and A. J. P. White (2010), Structural diversity in metal-organic frameworks built from rigid tetrahedral $[\text{Si}(p\text{-C}_6\text{H}_4\text{CO}_2)_4]^{4-}$ struts, *Crystal Growth & Design*, **10**, 4571-4581.S
- [13] L. Wen, P. Cheng and W. Lin (2012), Mixed-motif interpenetration and cross-linking of high-connectivity networks led to robust and porous metal-organic frameworks with high gas uptake capacities, *Chemical Science*, **3**, 2288-2292.
- [14] Q. Liu, X. Liu, H. Feng, H. Shui and R. Yu (2017), Metal organic frameworks-derived Fe/carbon porous composite with low Fe content for lightweight and highly efficient electromagnetic wave absorber J. Chemical Engineering Journal, **314**, 320-327.
- [15] S. S. Chen, R. Qiao, L. Q. Sheng, Y. Zhao, S. Yang, M. M. Cheng, Z. D. Liu and D. H L Wang (2013), Cadmium (II) and zinc (II) complexes with rigid 1-(1H-imidazol-4-yl)-3-(4H-tetrazol-5-yl) benzene and varied carboxylate ligands, *CrystEngComm*, **15**, 5713-5725.
- [16] D. M. L. Goodgame, P. D. Lickiss, S. J. Rooke, A. J. P. White and D. J. Williams (2003), Large-ring chain and sheet polymeric metal complexes of extended-reach siloxypyridine ligands $[\text{iPr}_2\text{SiO}(\text{CH}_2)_n\text{py}]_2$ *Inorganica Chimica. Acta*, **343**, 61-73.
- [17] D. M. L. Goodgame, P. D. Lickiss, S. J. Rooke, A. J. P. White and D. J. Williams (2001), Diversity of polymeric structures for copper complexes of the extended-reach siloxypyridine ligands $[\text{iPr}_2\text{SiO}(\text{CH}_2)_n\text{py}]_2$ (n= 0, 1, 3) *Inorganica Chimica. Acta*, **324**, 218-231.
- [18] G. Günay, O. Z. Yeşilel, H. Erer, S. Keskin and A. Tabak (2015), A zinc (II) metal organic framework based on flexible *o*-phenylenediacetate and rigid 4,4'-azobis (pyridine) ligands: synthesis, crystal structure and hydrogen gas adsorption properties *Polyhedron*, **100**, 108-113.

- [19] T. Mocanu, L. Pop, S. Shova, I. Grosu and M. Andruh (2017), Coordinating polymers constructed from tetrahedral-shaped adamantane tectons *CrystEngComm*, **19**, 27-31.
- [20] A. Schüttrumpf, E. Kirpi, A. Bulut, F. L. Morel, M. Ranocchiari, E. Lork, Y. Zorlu, S. Grabowsky, G. Yücesan and J. Beckmann (2015), Tetrahedral tetraphosphonic acids: New building blocks in supramolecular chemistry *Crystal Growth & Design*, **15**, 4925–4931.
- [21] J. Ai, X. Min, C. Y. Gao, H. R. Tian, S. Dang and Z. M. Sun (2017), A copper-phosphonate network as a high-performance heterogeneous catalyst for the CO₂ cycloaddition reactions and alcoholysis of epoxides, *Dalton Transaction*, **46**, 6756–6761.
- [22] J. K. Zaręba (2017), Tetraphenylmethane and tetraphenylsilane as building units of coordination polymers and supramolecular networks - A focus on tetraphosphonates *Inorganic Chemistry Communications*, **86**, 172–186.
- [23] A. D. G. Firmino, F. Figueira, J. P. C. Tomé, F. A. A. Paz and J. Rocha (2018), Metal-Organic Frameworks assembled from tetraphosphonic ligands and lanthanides *Coordination Chemistry Reviews*, **355**, 133–149.
- [24] S. E. Wenzel, M. Fischer, F. Hoffmann and M. Fröba (2009), High porous metal-organic Framework containing a novel organosilicon linker – a promising material for hydrogen storage *Inorganic Chemistry*, **48**, 6559–6565.
- [25] Y. Liu, J. Su, W. Li and J. Wu (2005), First hydrotalcite-like sulfonate coordination network incorporating robust cationic layers and flexible interlayer interactions *Inorganic Chemistry*, **44**, 3890–3895.
- [26] A. P. Côté and G. K. H. Shimizu (2004), Silver (I) arylsulfonates: a systematic study of “softer” hybrid inorganic-organic solids *Inorganic Chemistry*, **43**, 6663–6673.
- [27] Z. Wang and S. M. Cohen (2009), Postsynthetic modification of metal-organic frameworks *Chemical Society Reviews*, **38**, 1315-1329
- [28] J. Li, Y. Ma, M. C. McCarthy, J. Sculley, J. Yu, H. Jeong, P. B. Balbuena and H. Zhou (2011), Carbon dioxide capture-related gas adsorption and separation in metal-organic frameworks *Coordination Chemistry Reviews*, **255**, 1791-1823
- [29] D. G. Elizabeth Wilson, Carbon Capture and Sequestration: Integrating Technology, Monitoring and Regulation, John Wiley & Sons, US, 2007.
30. S. Nayak, H. P. Nayek, C. Pietzonka, G. Novitchi and S. Dehnen (2011), A series of three-dimensional lanthanide MOFs: observation of reversible structural changes controlled by solvent desorption-adsorption, and magnetic properties *Journal of Molecular Structure*, **1004**, 82-87